LES-INFORMED RESOLVENT-BASED ESTIMATION OF TURBULENT PIPE FLOW

Filipe R. Amaral and André V. G. Cavalieri
Department of Aerodynamics
Instituto Tecnológico de Aeronáutica
12228-900, São José dos Campos, SP, Brazil
filipefra@ita.br

ABSTRACT

A resolvent-based methodology is employed to obtain non-causal spatio–temporal estimates of turbulent pipe flow from low-rank probe measurements of wall shear-stress fluctuations. DNS and LES pipe flow numerical simulations at friction Reynolds number of 550 are used as databases. We consider one of the DNS databases as the true spatio–temporal flow field, from which the low-rank measurements are extracted. Such database is also employed to verify the accuracy of the linear estimators. The estimator needs a model for the nonlinear (or forcing) terms of the Navier-Stokes equations system, which are obtained from a DNS database and from a series of computationally cheaper LES databases with grids coarser than the DNS. Comparisons between the reference DNS and the estimates indicate that sufficiently accurate results can be achieved with cheaper LES containing up to 10% of the number of grid points of the DNS, with estimates closely matching the reference DNS results up to the buffer-layer and reasonable agreement up to the beginning of the log layer.

INTRODUCTION

The estimation of space–time flow fluctuations from noisy, low-rank measurements is an interesting option for the understanding of the turbulence physics and for the design of flow control strategies. For wall-bounded turbulent flows, wall quantities such as shear stress and/or pressure are usually employed as inputs for the estimation algorithms, as for practical applications the measurement of such quantities is easier to obtain than, e.g. the velocity components at a given distance from the wall. Model-based methodologies can be used to build the estimator (Bewley & Protas, 2004; Hœpffner *et al.*, 2005; Chevalier *et al.*, 2006; Colburn *et al.*, 2011; Illingworth *et al.*, 2018), although it is also possible to perform flow estimations based solely on data (Encinar & Jiménez, 2019; Sasaki *et al.*, 2019; Guastoni *et al.*, 2021). For both model- and data-driven methodologies the basic idea is to obtain relations between the measurements and the estimated flow state, but the model-based methodologies have the additional advantage of providing insight on the underpinning physics.

Linearized models can be obtained using the resolvent framework. In this case, the Navier-Stokes system is written in the state–space form and the nonlinear terms are interpreted as external forcing terms (McKeon & Sharma, 2010; Hwang & Cossu, 2010; Beneddine *et al.*, 2016; Taira *et al.*, 2017), hence providing an input–output formulation. Towne *et al.*

(2020) introduced a resolvent-based estimator for flow statistics, which was further generalized by Martini *et al.* (2020) for time-domain estimates. For the latter case, in order to build the transfer functions between the low-rank measurements and the flow state components, it is necessary to evaluate the resolvent operator and feed the algorithm with the cross-spectral density (CSD) of nonlinear terms, treated as forcing. If the true forcing CSD is used, optimal estimates of time-varying flow quantities are obtained. Such estimates are not causal, as the full time series of sensor data is required for estimation; extension to causal estimation, using only past sensor information, is proposed by (Martini *et al.*, 2022). Amaral *et al.* (2021) successfully applied the methodology by Martini *et al.* (2020) to direct numerical simulation (DNS) of turbulent channel flow, using wall shear-stress and pressure low-rank measurements. Results show a close agreement between estimates and reference DNS fluctuations in the near wall region, and good agreement for large scale structures throughout the channel. A key feature is the use of forcing statistics extracted from the DNS database, which leads to an optimal estimator but requires expensive simulation and post-processing to obtain the forcing CSD.

In the present paper we employ the aforementioned resolvent-based methodology to estimate the space–time velocity fluctuation components of turbulent pipe flow at friction Reynolds number $Re_\tau \approx 550$ using wall shear-stress measurements. In addition to DNS, we also explore the capability of wall-resolved large-eddy simulations (LES) to construct estimators. A first DNS database is used as the reference case from which we extract low-rank measurements of wall-shear stresses. A second DNS and the other LES databases provide the forcing (nonlinear) statistics to build the linear estimators. Here we investigate the capability of cheaper LES databases on the reconstruction of the space–time flow field, aiming to obtain a reliable and low-cost estimator that could be used for various high-Reynolds-number flows of practical interest.

METHODS
Resolvent-based estimator

We begin writing the linearized Navier-Stokes (LNS) equations in the discretized state-space form in time domain, i.e.

$$M\frac{d\boldsymbol{q}(t)}{dt} = \boldsymbol{A}\boldsymbol{q}(t) + \boldsymbol{B}\boldsymbol{f}, \tag{1a}$$

$$\boldsymbol{y}(t) = \boldsymbol{C}\boldsymbol{q}(t) + \boldsymbol{n}(t). \tag{1b}$$

In this equation, $q = \begin{bmatrix} u_x & u_r & u_\theta & p \end{bmatrix}^T$, where u_x, u_r and u_θ indicate streamwise, radial and azimuthal velocity fluctuations, respectively, and p indicates the pressure fluctuation. Moreover, t denotes time, A is the linearized Navier-Stokes operator, B is the actuation matrix that restricts the forcing terms to appear only in the momentum equation, y is the system observation (measurements), C is the observation matrix that selects N_s sensor readings from the state vector (in the present paper, wall-shear stresses in the axial and azimuthal directions), and n is the measurement noise. M is a diagonal matrix whose entries are set to one and zero for the momentum and continuity equations, respectively. Dependency on longitudinal and azimuthal wavenumbers, α and m, respectively, as well as on wall-normal variable y, were dropped to simplify notations. For pipe flow, the LNS operator $L = (-i\omega M - A)$ is written in cylindrical coordinates (Luhar *et al.*, 2014) and linearization is around the mean turbulent profile, considered as known.

Equation 1 can be written in the frequency domain as

$$\hat{y}(\omega) = \left[C(-i\omega M - A)^{-1} B \right] \hat{f}(\omega) + \hat{n}(\omega), \qquad (2)$$

where ω denotes frequency and hats are used for Fourier-transformed quantities. Following (Martini *et al.*, 2020), it is possible to obtain the optimal linear transfer function ($\hat{T}_q$) between the system observation ($\hat{y}$) and the estimated flow state components ($\hat{\tilde{q}}$), i.e.

$$\hat{\tilde{q}} = \hat{T}_q \hat{y}, \qquad (3)$$

where $\hat{T}_q$ is the transfer function and dependency on frequency ω was dropped to simplify notations. Martini *et al.* (2020) derived a expression for $\hat{T}_q$ that is based on the minimization of the error between the true ($\hat{f}$) and estimated ($\hat{\tilde{f}}$) forcing terms and is given by

$$\hat{T}_q = RBP_{ff}H^* \left(HP_{ff}H^* + P_{nn} \right)^{-1}, \qquad (4)$$

where $R = (-i\omega M - A)^{-1}$ is the resolvent operator, $H = CRB$ is the resolvent operator including the observation (C) and actuation (B) matrices, $P_{nn} = \langle \hat{n}\hat{n}^* \rangle$ and $P_{ff} = \langle \hat{f}\hat{f}^* \rangle$ are CSDs of sensor noise and forcing, respectively. The asterisk ($*$) indicates a Hermitian transpose. More details on the estimator derivation can be found in Martini *et al.* (2020).

To build the transfer function (Eq. 4), it is necessary to specify *a priori* the forcing CSD (P_{ff}). When true forcing statistics are known, Eq. 4 provides the optimal linear estimator. Other models for the forcing CSD provide sub-optimal estimators.

The snapshots are reconstructed according to the procedures described in Amaral *et al.* (2021) and are briefly addressed below. First, it is necessary to take the inverse Fourier transform of the transfer function $\hat{T}_q$, Eq. 4, in order to return to time domain and obtain T_q. Hence, the time domain transfer function T_q must be convolved with the measurements/observations $y(t)$ to evaluate the state estimate in time domain $\tilde{q}$. Finally, double inverse Fourier transforms in the azimuthal and longitudinal directions are taken in order to return from wavenumber domain to physical space.

Numerical simulations

To generate the databases, we employed numerical simulations conducted with the Openpipeflow code (Willis, 2017).

Periodic boundary conditions were assumed in the streamwise and azimuthal directions. For all simulations the pipe length is $L_z = 10R$, where R is the pipe radius. Table 1 shows the parameters for all cases, including the number of streamwise (N_z) and azimuthal wavenumbers (N_θ), the number of mesh points in the radial direction (N_r), the mesh discretization in the streamwise (Δz^+), azimuthal (($R\Delta\theta)^+$) and radial (Δy^+) directions and the mesh points ratio with respect to the DNS case (N/N_{DNS}). Plus symbols denote inner (wall and/or viscous) units. All simulations contain 2981 snapshots and the time steps based on outer units is $\Delta t = 0.2$ for all simulations. Cases starting with D denote DNS, whereas letter L indicate LES, carried out using (Smagorinsky, 1963) subgrid scale model, with a Smagorinsky constant set as $C_s = 0.05$. As estimations lose accuracy for large wavenumbers, only the lowest 16 and 32 streamwise and azimuthal wavenumbers were used to construct the estimators. Welch's method (Welch, 1967) was employed to evaluate the forcing and state components statistics, with blocks containing $N_{fft} = 256$ time steps and 75% overlap. A Hann window was applied to each block to minimize spectral leakage.

The simulations were validated with reference DNS results by El Khoury *et al.* (2013) (not shown here). Cases D1, D2 and L1 show good agreement with the reference simulations, regarding mean flow profile, axial, azimuthal and radial velocity fluctuations. The coarser grid cases (L3, L6 and L8) progressively deteriorate the agreement, with the L8 case showing strong mismatch with all quantities.

Wall shear-stress measurements in the axial and azimuthal directions were extracted from the D1 database, which is taken as ground truth. The other databases, i.e. D2, L1, L3, L6 and L8, were employed to construct the estimator transfer functions by extracting the forcing statistics (P_{ff}). It is important to remark that the estimators employed in this study have no information from the D1 case. The LES databases, which have coarser grids, significantly reduce the estimates computational cost, since the number of grid points to run the simulations are small, but in turn lead to suboptimal estimators. In this paper we employ P_{ff} obtained in simulations that have different grids than the measurements database (D1) and after the evaluation of the transfer functions results are interpolated to a grid equivalent to that of the measurement database.

RESULTS

Figures 1, 2 and 3 show sample snapshots of the streamwise velocity fluctuations from the D1 database, filtered to retain only the lower axial and azimuthal wavenumbers, and corresponding estimates obtained using D2, L1, L3, L6 and L8 forcing statistics. Results are shown at radial distances from the pipe wall of $y^+ = (1 - r^+) \approx 15$ and 100 and 200. Plus superscripts denote inner (viscous) scaling units, r is the radial coordinate and y is the distance from the pipe wall. In the figures we use a pseudo-spanwise coordinate $z = r\theta$ ($\lambda_z = r\lambda_\theta$) for enabling comparisons with structures found in planar wall-bounded flows.

When considering the buffer layer, at a wall-normal distance of $y^+ \approx 15$, the resemblance between DNS results and the estimates is remarkable, even when the L8 forcing is employed. This is somehow expected, since (Amaral *et al.*, 2021) showed that assuming the forcing statistics as spatial white noise to build the estimator also provides accurate estimates for distances very close to the wall. Moving further from the wall, the estimates are not as accurate, especially for the coarser LES (L8) estimator, although most of the large-scale

Table 1: DNS and LES numerical simulations parameters.

Case	Re_τ	N_r	N_z	N_θ	Δz^+	$(R\Delta\theta)^+$	Δy^+	N/N_{DNS}
D1	550.3	128	528	528	10.4	6.5	0.07-6.3	1.000
D2	550.3	128	528	528	10.4	6.5	0.07-6.3	1.000
L1	548.5	96	384	384	14.2	8.9	0.4-14.7	0.397
L3	568.6	96	192	192	28.6	18.0	0.4-15.2	0.099
L6	551.8	64	64	64	86.1	54.1	0.7-22.9	0.007
L8	509.6	32	32	32	159.3	100.1	0.7-22.9	0.002
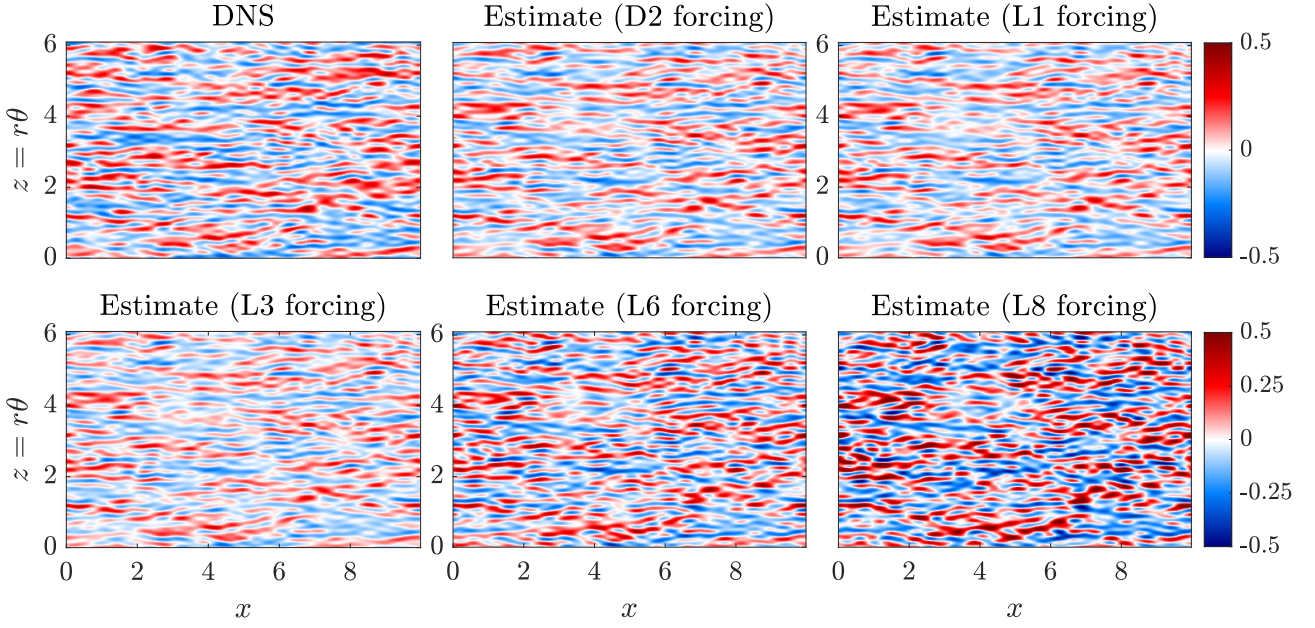
Figure 1: Comparison between streamwise velocity component instantaneous snapshot of filtered DNS (D1) and resolvent-based estimates using wall measurements of shear stress and considering the D2, L1, L3, L6, and L8) forcing statistics at $y^+ \approx 15$. Fluctuations shown in outer units.
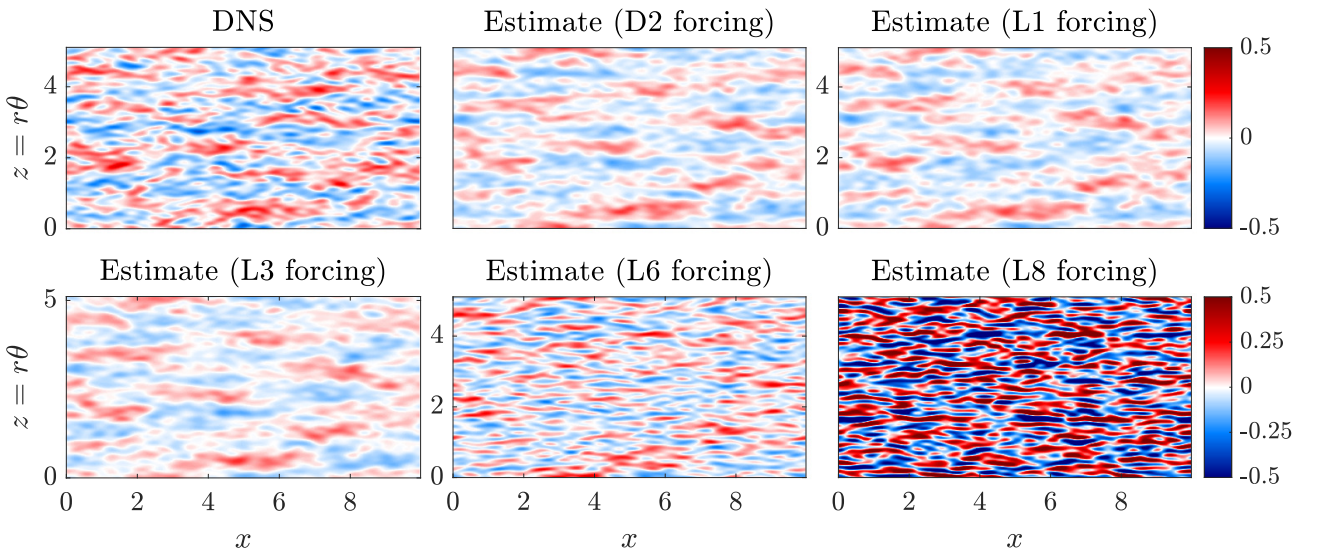
Figure 2: Comparison between streamwise velocity component instantaneous snapshot of filtered DNS and resolvent-based estimates at $y^+ \approx 100$. See comments in the caption of figure 1.

3
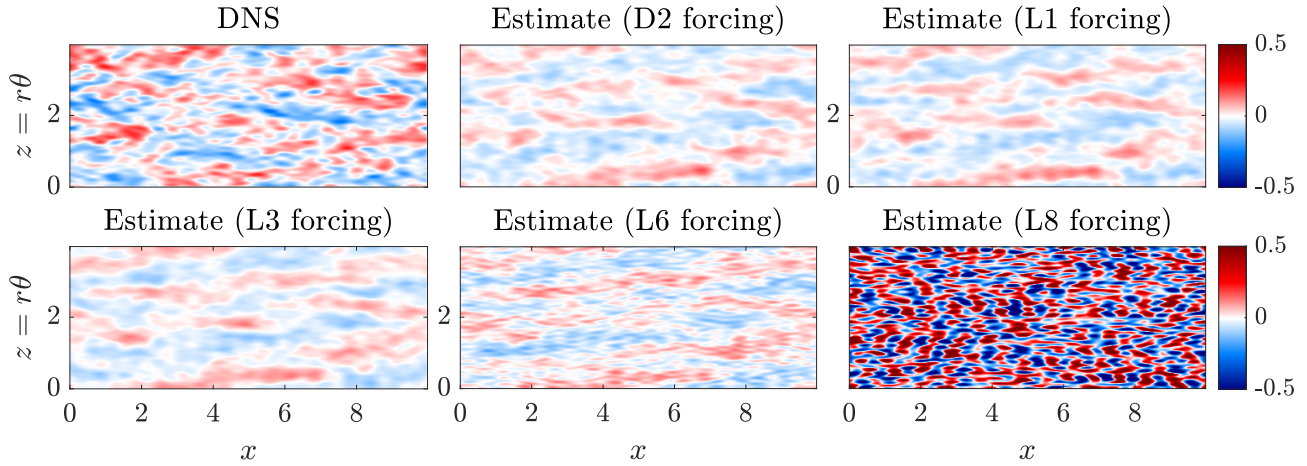
Figure 3: Comparison between streamwise velocity component instantaneous snapshot of filtered DNS and resolvent-based estimates at $y^+ \approx 200$. See comments in the caption of figure 1.

structures present in the DNS snapshots are still recognizable in all but the L8 estimator. Regarding the radial and azimuthal velocity components, not shown here, similar results as those of the streamwise velocity component were observed.

Figure 4 displays normalized correlations (*Corr*, left frame), r.m.s errors (*Err*, middle frame) and variance ($\langle q'q' \rangle^+$, right frame) for the streamwise velocity component. Such metrics are defined in Amaral *et al.* (2021) and, for brevity, we refer to this paper for further details on the metrics definitions. Accurate estimates correspond to low normalised error *Err*, close to 0, and high correlation *Corr*, close to 1.

All estimators are accurate up to $y^+ \approx 10$, showing correlation and r.m.s. errors of approximately 0.95 and 0.35, respectively. Moving farther from the wall, only estimators D2, L1 and L3 remain accurate, especially regarding the correlation and r.m.s. metrics. It is interesting that estimator L3, which has a grid with less than 10% of the points used for the DNS-based estimator, could attain such accuracy. This indicates that the large scales of interested are well calculated in the LES, as expected, and their statistics may be used to build an accurate estimator at a fraction of the computational cost of the DNS-based estimator considered in Amaral *et al.* (2021). L6 and L8 estimators, on the other hand, provided results that are comparable to cases including eddy-viscosity model on the linear operator and white-noise forcing statistics modelling, strategies that our group previously employed to obtain estimates of channel flow after low-tank measurements (Amaral *et al.*, 2021). Overall, the quantitative metrics in figure 4 confirm the qualitative results shown in figures 1-3. Similar results, not shown here, were obtained for the azimuthal and radial velocity components.

Normalized r.m.s. error as a function of the wavenumbers for the studied estimators are shown in figure 5 for wall distances (planes) of $y^+ \approx 15$ and 100. The large structures, which are characterised by small α and m, are accurately estimated for the D2, L1 and L3 cases, with virtually zero r.m.s. error at both planes. The estimates for smaller structures (large α and m), on the other hand, display higher r.m.s. error, especially for the $y^+ \approx 100$ plane. For the coarser L6 and L8 estimators, even for the $y^+ \approx 15$ plane, the accuracy of smaller structure estimates is quite low.

CONCLUSIONS

In this paper we employed resolvent-based estimators to obtain the space–time flow field of turbulent pipe flow from wall-shear stress measurements. We compared the performance of the estimator when modelling the forcing terms with DNS and LES databases. Satisfactory results were obtained with the forcing statistics from LES, especially up to the buffer layer. The accuracy level of a LES estimator containing approximately 10% of the grid points of the DNS database is very close to what is obtained with the DNS estimator. LES-informed resolvent-based estimation is thus a viable approach for accurate estimates of turbulent flow at high *Re*.

Acknowledgements

REFERENCES

Amaral, Filipe Ramos, Cavalieri, André Valdetaro Gomes, Martini, Eduardo, Jordan, Peter & Towne, Aaron 2021 Resolvent-based estimation of turbulent channel flow using wall measurements. *Journal of Fluid Mechanics* **927**, A17.

Beneddine, Samir, Sipp, Denis, Arnault, Anthony, Dandois, Julien & Lesshafft, Lutz 2016 Conditions for validity of mean flow stability analysis. *Journal of Fluid Mechanics* **798**, 485–504.

Bewley, Thomas R. & Protas, Bartosz 2004 Skin friction and pressure: the "footprints" of turbulence. *Physica D: Nonlinear Phenomena* **196** (1-2), 28–44.

Chevalier, Mattias, Hœpffner, Jérôme, Bewley, Thomas R. & Henningson, Dan S. 2006 State estimation in wall-bounded flow systems. Part 2. Turbulent flows. *Journal of Fluid Mechanics* **552** (1), 167.

Colburn, C. H., Cessna, J. B. & Bewley, T. R. 2011 State estimation in wall-bounded flow systems. Part 3. The ensemble Kalman filter. *Journal of Fluid Mechanics* **682**, 289–303.

El Khoury, George K., Schlatter, Philipp, Noorani, Azad, Fischer, Paul F., Brethouwer, Geert & Johansson, Arne V. 2013 Direct Numerical Simulation of Turbulent Pipe Flow
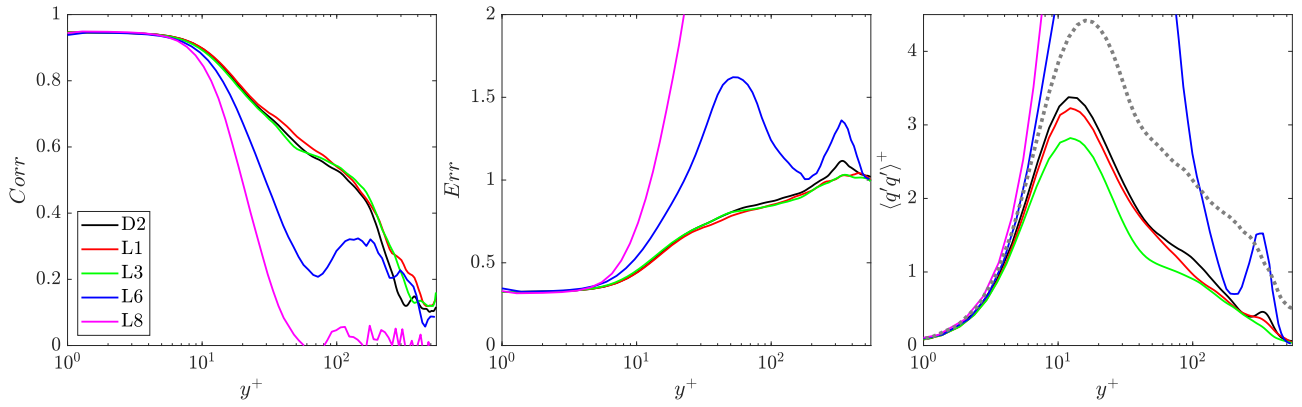
Figure 4: Flow state comparison metrics for the streamwise velocity fluctuation component. Dash-dotted grey curve in the left frame denote DNS (D1) results. Frames, from left to right: correlation, normalized r.m.s. and variance. The DNS variance refers solely to wavenumbers retained for estimation.
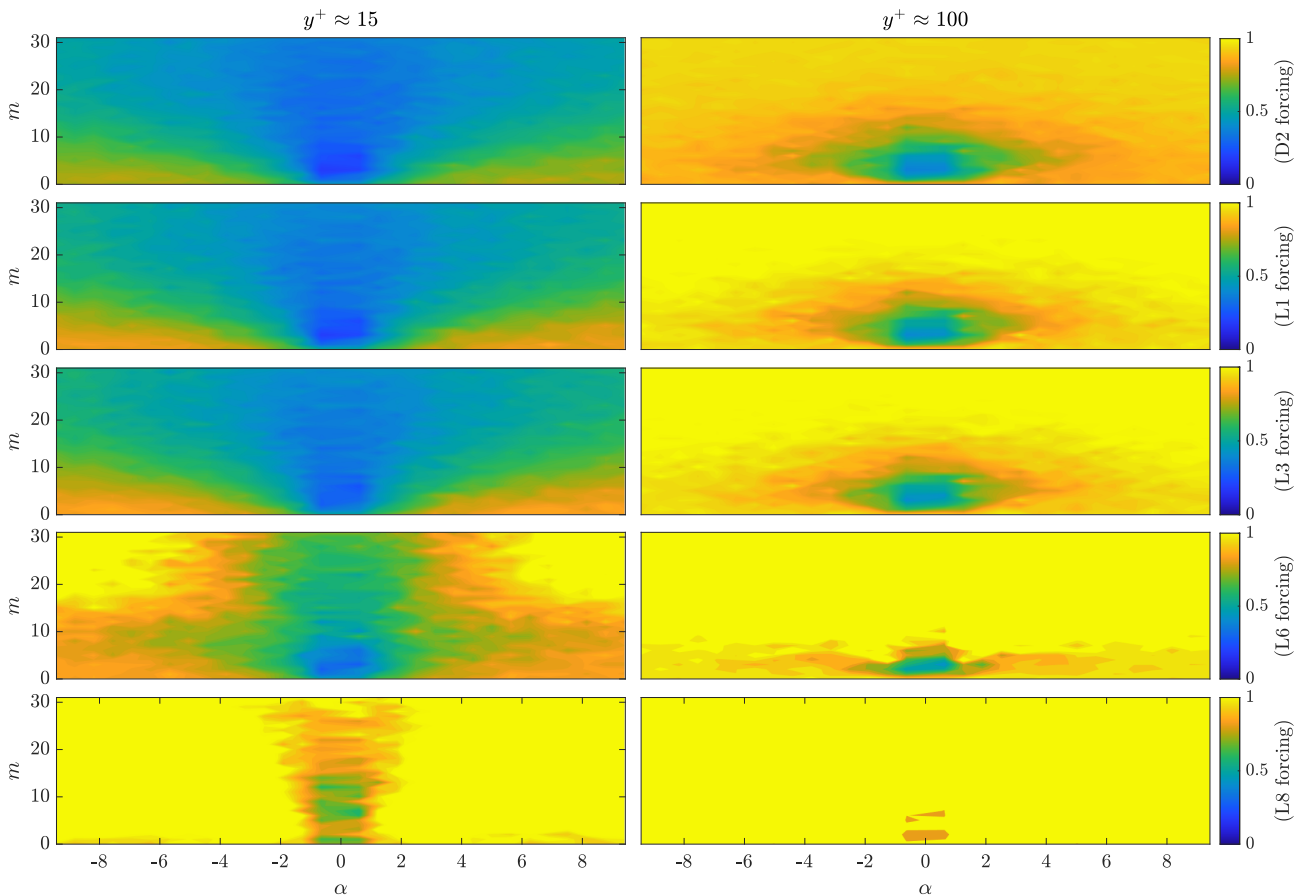
Figure 5: Normalized r.m.s. error as a function of (α,m) state comparison metrics for D2, L1, L3, L6 and L8 estimators.

at Moderately High Reynolds Numbers. *Flow, Turbulence and Combustion* **91** (3), 475–495.

Encinar, Miguel P. & Jiménez, Javier 2019 Logarithmic-layer turbulence: A view from the wall. *Physical Review Fluids* **4** (11), 114603.

Guastoni, Luca, Güemes, Alejandro, Ianiro, Andrea, Discetti, Stefano, Schlatter, Philipp, Azizpour, Hossein & Vinuesa, Ricardo 2021 Convolutional-network models to predict wall-bounded turbulence from wall quantities. *Journal of Fluid Mechanics* **928**, A27.

Hœpffner, Jérôme, Chevalier, Mattias, Bewley, Thomas R. & Hennington, Dan S. 2005 State estimation in wall-bounded

flow systems. Part 1. Perturbed laminar flows. *Journal of Fluid Mechanics* **534**, 263–294.

Hwang, Yongyun & Cossu, Carlo 2010 Linear non-normal energy amplification of harmonic and stochastic forcing in the turbulent channel flow. *Journal of Fluid Mechanics* **664**, 51–73.

Illingworth, Simon J., Monty, Jason P. & Marusic, Ivan 2018 Estimating large-scale structures in wall turbulence using linear models. *Journal of Fluid Mechanics* **842**, 146–162.

Luhar, Mitul, Sharma, Ati S. & McKeon, Beverley J. 2014 Opposition control within the resolvent analysis framework. *Journal of Fluid Mechanics* **749**, 597–626.

Martini, Eduardo, Jordan, Peter, Cavalieri, André V. G., Towne, Aaron & Lesshafft, Lutz 2020 Resolvent-based optimal estimation of transitional and turbulent flows. *Journal of Fluid Mechanics* **900**, A2.

Martini, Eduardo, Jung, Junoh, Cavalieri, André V. G., Jordan, Peter & Towne, Aaron 2022 Resolvent-based tools for optimal estimation and control via the Wiener-Hopf formalism. *Journal of Fluid Mechanics (accepted)* **937**, A19.

McKeon, B. J. & Sharma, A. S. 2010 A critical-layer framework for turbulent pipe flow. *Journal of Fluid Mechanics* **658**, 336–382.

Sasaki, Kenzo, Vinuesa, Ricardo, Cavalieri, André V. G., Schlatter, Philipp & Henningson, Dan S. 2019 Transfer functions for flow predictions in wall-bounded turbulence. *Journal of Fluid Mechanics* **864**, 708–745.

Smagorinsky, Joseph 1963 General circulation experiments with the primitive equations: I. The basic experiment. *Monthly Weather Review* **91** (3), 99–164.

Taira, Kunihiko, Brunton, Steven L., Dawson, Scott T. M., Rowley, Clarence W., Colonius, Tim, McKeon, Beverley J., Schmidt, Oliver T., Gordeyev, Stanislav, Theofilis, Vassilios & Ukeiley, Lawrence S. 2017 Modal analysis of fluid flows: An overview. *AIAA Journal* **55** (12), 4013–4041.

Towne, Aaron, Lozando-Durán, Adrián & Yang, Xiang 2020 Resolvent-based estimation of space–time flow statistics. *Journal of Fluid Mechanics* **883**, A17.

Welch, Peter D. 1967 The use of Fast Fourier Transform for the estimation of power spectra: A method based on time averaging over short, modified periodograms. *IEEE Transactions on Audio and Electroacoustics* **15** (2), 70–73.

Willis, Ashley P. 2017 The Openpipeflow Navier–Stokes solver. *SoftwareX* **6**, 124–127.